Single-Image Diffusion Coefficient Measurements of Proteins in Free Solution

Shannon Kian Zareh,[†△] Michael C. DeSantis,[†△] Jonathan M. Kessler,[†] Je-Luen Li,[‡] and Y. M. Wang[†*]
[†]Department of Physics, Washington University in St. Louis, Saint Louis, Missouri; and [‡]D. E. Shaw Research, New York, New York

ABSTRACT Diffusion coefficient measurements are important for many biological and material investigations, such as studies of particle dynamics and kinetics, and size determinations. Among current measurement methods, single particle tracking (SPT) offers the unique ability to simultaneously obtain location and diffusion information about a molecule while using only femtomoles of sample. However, the temporal resolution of SPT is limited to seconds for single-color-labeled samples. By directly imaging three-dimensional diffusing fluorescent proteins and studying the widths of their intensity profiles, we were able to determine the proteins' diffusion coefficients using single protein images of submillisecond exposure times. This simple method improves the temporal resolution of diffusion coefficient measurements to submilliseconds, and can be readily applied to a range of particle sizes in SPT investigations and applications in which diffusion coefficient measurements are needed, such as reaction kinetics and particle size determinations.

INTRODUCTION

It is important to determine the diffusion coefficients of particles for many biological and material applications, such as single-molecule dynamics studies (1–3), biochemical and pharmaceutical reaction kinetics studies (4,5), and particle size and shape determinations (6). Among current methods for measuring diffusion coefficients, such as NMR (7), dynamic light scattering (8), fluorescence correlation spectroscopy (FCS) (9–11), and fluorescence recovery after photobleaching (FRAP) (12), the technique known as single-particle tracking (SPT) offers the unique ability to determine location and diffusion coefficients simultaneously. This is essential for molecular mechanism investigations in heterogeneous environments such as inside a cell's cytoplasm (13) or flagella (14), a membrane in vivo (15), and on a DNA molecule (1) in vitro. Because of this capability, and the additional advantage that SPT experiments require less than femtomoles of sample, SPT can be a powerful tool for measuring diffusion coefficients in a large number of biological investigations (in vitro and in vivo) in which supplies are scarce.

However, the drawback of using SPT for diffusion coefficient measurements is the low temporal resolution. In single-molecule fluorescence imaging studies, stationary or slowly moving (relative to the data-acquisition timescales) single-molecule intensity profiles are called point spread functions (PSFs), and are fit to Gaussian functions to determine the molecules' localization information. The centroid of the Gaussian function determines the lateral location of the molecule at the time of imaging, and the standard deviation (SD) determines the axial location. In SPT diffusion coefficient measurements, consecutive locations of a single fluorophore are measured, and diffusion coefficients are obtained from mean-square displacement analysis of the particle's single trajectories (1,13,16). This method requires at least 20 consecutive location measurements for each single trajectory. With the current single-photon camera imaging rate of ~100 frames/s for a finite-sized imaging area, 0.2 s is required, and three-dimensional (3D) diffusion coefficient (D_{3D}) measurements up to order 10^5 nm^2/s have been reported (17). However, this requirement of 0.2 s is too long for diffusion coefficient measurements of fast-moving molecules, such as nanometer-sized proteins that diffuse beyond the typical imaging depth of ~400 nm of single-molecule imaging microscope setups in $<$1 ms (a typical 5 nm protein has $D_{3D} \approx 10^8$ nm^2/s and diffuses $\sqrt{2D_{3D}t} \approx 447$ nm in 1 ms). A recently developed SPT method measures D_{3D} up to 1.7×10^7 nm^2/s by labeling the particles with two colors (18); however, multicolor labeling may not be feasible for many biological particles of interest, which restricts the applicability of the method.

A SPT method that can determine 3D diffusion coefficients of single-colored nanometer-sized biological entities in their native environment is highly desirable for in vivo and in vitro studies. For the molecule to be captured within the microscope's imaging depth, the imaging time must be $<$1 ms. Here we report a novel (to our knowledge) method that can be used to determine the diffusion coefficient of nanometer-sized Brownian molecules from the SD values of the molecules' intensity profiles using submillisecond exposure times. This single-image molecular analysis (SIMA) study of dynamic molecules is an extension of our previous stationary molecule investigations

Submitted November 9, 2011, and accepted for publication February 13, 2012.

△Shannon Kian Zareh and Michael C. DeSantis contributed equally to this work.

*Correspondence: ymwang@wustl.edu

Editor: Taekjip Ha.

0006-3495/12/04/1685/7 $2.00

doi: 10.1016/j.bpj.2012.02.030

(19). In this study, we used enhanced green fluorescent protein (eGFP) as the nanometer-sized fluorescent molecule for measurements and analyses.

Because the imaging times in our method are <1 ms, the temporal resolution of the diffusion coefficient measurements is improved by at least 1000-fold over the minutes-long FCS method (multiple measurements, each ~20 s long), 200-fold over the 0.2-s-long centroid SPT method, 50-fold over the typically 50-ms-long FRAP method, and 10-fold over the two-color SPT method. Furthermore, the improvement in temporal resolution is achieved without compromising the precision of the D_{3D} measurements, and the single-image nature of the method avoids the photobleaching and limited lifetime photon problems associated with single-molecule fluorescence imaging studies. Below, we describe our measurement method, which relates the SD of a 3D freely diffusing protein's intensity profile to its diffusion coefficient D_{3D}. In a previous study, Schuster et al. (20) used a similar concept to relate slow 2D diffusion coefficients (up to 1.1×10^6 nm^2/s with a temporal resolution > 25 ms) to a fluorophore's spot sizes. Here, we extend that study to fast 3D diffusions (D_{3D} up to $>10^8$ nm^2/s and temporal resolutions < 1 ms). By providing the 2D to 3D modification, and the explicit conditions for measuring particles of different sizes (i.e., the appropriate exposure time for a particular particle size; see Appendix S1 and Appendix S2 in the Supporting Material), our study allows for D_{3D} determination of different-sized particles in their native solvents.

MATERIALS AND METHODS

Sample preparation and imaging

eGFP molecules (4999-100; BioVision, Mountain View, CA) were diluted in 0.5× TBE buffer (45 mM Tris, 45 mM boric acid, 1 mM EDTA, pH 8.0) to 0.03 nM. For stationary eGFP studies, manufacturer-precleaned fused-silica chips (6W675-575 20C; Hoya, San Jose, CA) were used, and isolated eGFP molecules were adsorbed to surfaces at low concentration. For diffusing eGFP studies, the manufacturer-precleaned fused-silica chips were treated with oxygen plasma for 3 min, rendering them hydrophilic to prevent eGFP adsorption (21). The hydrophilic fused-silica surface can be considered ballistic for the diffusing eGFP molecules in our experiments and simulations. For both studies, a protein solution of 5 μL was sandwiched between the fused-silica surface and an oxygen-plasma-cleaned coverslip (2.2×2.2 cm^2), resulting in a 10.5-μm-thick water layer. Because the oxygen-plasma-treated fused-silica surface is hydrophilic, the buffer quickly wetted the surface and bubbles were rarely observed. The coverslip edges were then sealed with nail polish to prevent possible stray flow of the buffer due to evaporation.

Single-molecule imaging was performed on a Nikon Eclipse TE2000-S inverted microscope (Nikon, Melville, NY) in combination with a Nikon 100× objective (1.49 N.A., oil immersion). The samples were excited by prism-type total internal reflection fluorescence (TIRF) microscopy with a linearly polarized 488 nm laser line (I70C-SPECTRUM argon/krypton laser; Coherent, Santa Clara, CA) focused on a 40×20 μm^2 region. The 488 nm line was filtered from the multiline laser emission with the use of polychromatic acousto-optic filters (48062 PCAOM model; NEOS Technologies, Melbourne, FL). The laser excitation was pulsed with an illumination interval of 30 ms for the stationary eGFP molecules shown in Fig. 1 and Fig. S2, and between 0.3 and 1 ms for the diffusing eGFP molecules. The excitation intensities were 2.7 and 3.2 kW/cm^2 for the respective stationary eGFP molecules, and 37.5 kW/cm^2 for the diffusing molecules. Images were captured by an iXon back-illuminated electron multiplying charge coupled device (EMCCD) camera (DV897ECS-BV; Andor Technology, Belfast, Northern Ireland). An additional 2× expansion lens was placed before the EMCCD, producing a pixel size of 79 nm. The excitation filter was 488 nm/10 nm, and the emission filter was 525 nm/50 nm.

Data acquisition and selection

We obtained movies by synchronizing the onset of camera exposure with laser illumination for different intervals. The maximum gain level of the camera was used and the data acquisition rate was 1 MHz pixels/s (≈3.3 frames/s). We checked the single-molecule images to ensure that there were no saturations in the intensity profiles. For the defocusing analysis of stationary eGFP molecules, we selected 21 × 21 pixel boxes centered at the molecule by hand using ImageJ (NIH, Bethesda, MD), and used the intensity values for 2D Gaussian fitting. For the diffusing eGFP molecule movies, we selected all visible diffusing eGFP intensity profiles in the peak laser excitation region of 10×10 μm^2 by hand using 39×39 pixel boxes centered at the molecule. The center 25×25 pixels of the boxes were used for 2D Gaussian fitting, and the peripheral pixels were used for experimental background analysis.

Before performing the analysis, we converted the camera's intensity count at each pixel in an image into the photon count by using the camera-to-photon count conversion factor calibrated the same day of the measurement, as described in our previous article (22). We obtained the number of detected photons in an image by subtracting the total photon count of the background from the total photon count of the image. The eGFP intensity profiles were fit to a 2D Gaussian function to obtain the SD values of the molecule:

$$f(x,y) = f_0 \exp\left[-\frac{(x-x_0)^2}{2s_x^2} - \frac{(y-y_0)^2}{2s_y^2}\right] + \langle b\rangle, \quad (1)$$

where f_0 is the multiplication factor; s_x and s_y are SDs in the x and y directions, respectively; x_0 and y_0 are the centroid location of the molecule; and $\langle b\rangle$ is the mean background offset in photons.

For the defocusing eGFP analysis, we selected 17 adsorbed eGFP molecules with a minimum photon count of 229 and signal/noise ratios (SNRs, $I_0/\sqrt{I_0+\sigma_b^2}) > 3.75$, where I_0 is the peak PSF photon count (after subtracting the mean background offset $\langle b\rangle$) and σ_b^2 is the background variance in photons. For the diffusing eGFP molecules, we used an SNR of 2.5 as a selection criterion. We did not use PSFs with photon counts of <50 in the analysis. At each exposure time, we acquired 1600 data points from four movies (two acquired at different regions of an imaging chip on the same day, and two acquired from different chips on other days). The numbers of diffusing eGFP data used for the experimental analysis that satisfied the SNR criteria were 419–1066 for the 0.3–1 ms exposure times, respectively.

Diffusing eGFP simulations

We simulated 3D Brownian diffusion eGFP trajectories at a range of exposure times using FCS-determined eGFP $D_{3D} = 8.86 \times 10^7$ nm^2/s and triplet-state statistics. The starting locations of the trajectories followed the distribution function described in Appendix S6. The step sizes in the x, y, and z directions were randomly selected from a Gaussian distribution with a mean of zero and SD of $\sqrt{2D_{3D}t_0}$ with a step time $t_0 = 1$ μs. Because of the reflective fused-silica-water interface, the simulated z-values were

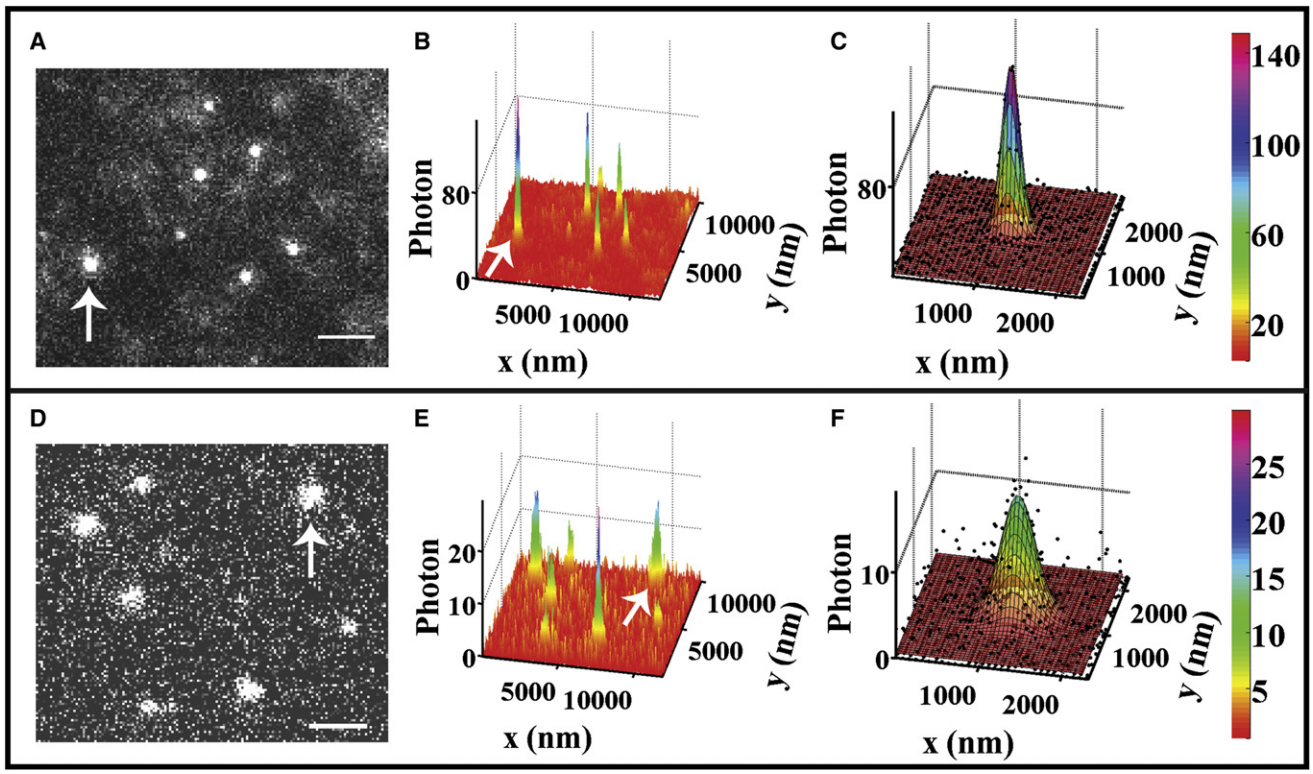

FIGURE 1 Comparison of stationary and diffusing eGFP molecules. (*A*) An image of stationary eGFP molecules adsorbed on a fused-silica surface. Five of the seven molecules have SNR > 2.5. (*B*) Intensity profiles of the stationary eGFP molecules in panel *A* in photon counts. (*C*) Intensity profile (*dots*) and Gaussian fit (*mesh*) to the stationary eGFP molecule denoted by arrow in *A* and *B*. For this molecule, the SNR is 9.8, $s_x = 107.2$ nm, and $s_y = 107.9$ nm. (*D*) Diffusing eGFP molecules near a reflective hydrophilic fused-silica surface at 1 ms exposure time. Six of the eight molecules have a SNR > 2.5. The scale bars for *A* and *D* are 2 μm. (*E*) Intensity profiles of the diffusing eGFP molecules in *D*. (*F*) Intensity profile (*dots*) and Gaussian fit (*mesh*) to the diffusing eGFP molecule denoted by the arrows in *D* and *E*. For this molecule, the SNR is 3.5, $s_x = 202.2$ nm, and $s_y = 192.4$ nm. It is clear that the intensity profiles of diffusing molecules are wider (or have larger SDs) than those of stationary molecules.

maintained above zero. The number of steps in a simulation was t / t_0. At each x, y location in a trajectory, when the molecule was not in a triplet dark state, a Poisson distributed number of photons (Appendix S5) was drawn from a Gaussian PSF spatial distribution with a mean of zero and the corresponding SD value for the axial location (Appendix S4). We added this relative displacement of the photons to the simulated x, y location of the molecule, generating the actual x, y location of the emitted photons at the simulation step.

The simulated photons of each trajectory were binned into 50×50 pixels with a pixel size of 79 nm. We then converted the photon count of each pixel into the modified camera count using Eq. 4 of DeSantis et al. (22), with the photon multiplication factor of the camera set at $M = 1$ to include the camera count variance effect. We generated random background photons at each pixel using the corresponding experimental background distribution functions for the exposure time (22). The final intensity profiles were fit to a 2D Gaussian function to obtain the two SD values for the image. For each SD datum of diffusing eGFP molecules shown in Fig. 5, 1000 independent trajectories were simulated.

RESULTS

Figs. 1 and 2 illustrate the principle of this method. In a finite exposure time, the intensity profile of a moving molecule is wider (or more blurry) than that of an immobile molecule. Fig. 1 *A* shows a 30-ms frame image of stationary eGFP molecules adsorbed on a fused-silica surface, and Fig. 1 *D* shows a 1-ms frame image of diffusing eGFP molecules near a hydrophilic fused-silica surface (21). These figures clearly show that the diffusing-molecule images are blurry compared with the immobile-molecule images. In Fig. 1, *B* and *E*, the intensity profiles of the stationary and diffusing eGFP molecules are plotted, and in Fig. 1, *C* and *F*, the respective selected intensity profiles are fitted to Gaussian functions. Although both intensity profiles fit well to a Gaussian function, the width (or SD) of the diffusing protein's intensity profile is larger than that of the stationary protein.

In general, the final image of a diffusing molecule, such as those in Fig. 1, is the sum of the emitted photons along its diffusion trajectory projected onto a 2D imaging screen. Fig. 2 *A* shows a simulated eGFP diffusion trajectory at 0.6-ms exposure time using 0.005 ms steps for clarity. The data are grayscaled to correspond to the particle's axial locations (Appendix S5). The emitted photons, after photon-to-camera count conversion, were projected onto a 2D imaging screen and binned into our camera pixels (each 79×79 nm^2 in size; Fig. 2 *B*, bottom, *gray image*), and the corresponding diffusing eGFP PSF intensity profile was formed in the colored image above. The total photon count

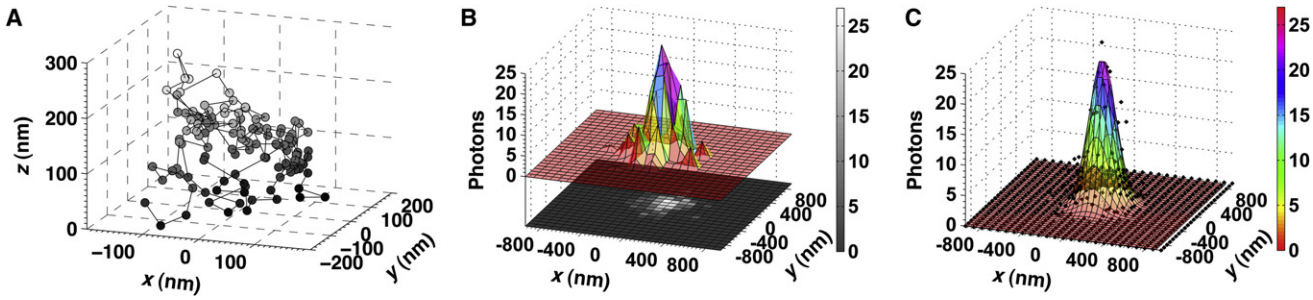

FIGURE 2 Simulated image formation and analysis process of a diffusing eGFP molecule. (*A*) Trajectory of a diffusing eGFP molecule in free solution under TIRF evanescent excitation at the exposure time of 0.6 ms. The data are grayscaled to correspond to the particle's axial locations (Appendix S5). (*B*) The emitted photons from the trajectory form an intensity profile (*top*, *colored plot*), which is then projected onto a 2D camera screen (*bottom*, *black and white image*). (*C*) Gaussian fit (*mesh*) to the intensity profile of the diffusing eGFP (*dots*), where $s_x = 119.4$ nm, and $s_y = 142.2$ nm.

of this image was 414. The 2D Gaussian fit to the diffusing eGFP intensity profile is shown in Fig. 2 *C*, yielding SD values in the x and y directions. The $s_{x,y}$-values presented in this article are the results from fitting to these experimental and simulated PSF data, and were used to quantify the blur of diffusing eGFP molecules and consequently the diffusion coefficient D_{3D}.

To determine D_{3D} from diffusing fluorophore images, we performed experimental measurements, analytical calculations, and simulations. Below, we show that when we checked the experimental results against the theoretical calculation and numerical simulation results, we obtained good agreement, which validates our method of measuring nanometer-sized fluorophore diffusion coefficients.

Fig. 3 *A* shows representative eGFP images (chosen such that the molecule's respective s_x-values were within ± 5 nm of the means to the respective diffusing eGFP intensity profile SD distributions in Fig. 3 *B*) acquired at 0.3, 0.7, and 1 ms exposure times in experimental measurements. As expected, the SD values of these respective single diffusing eGFP molecules increase from 136.4 to 160.9

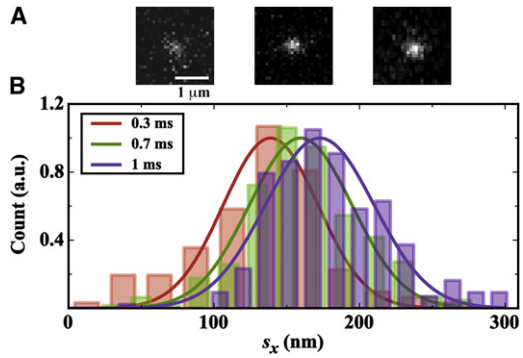

FIGURE 3 Diffusing eGFP images and intensity profile SD distributions at different exposure times. (*A*) Three representative images showing diffusing eGFP molecules at exposure times of 0.3, 0.7, and 1 ms. The intensity profile SD values increase with the exposure time. The scale bar is 1 μm. (*B*) EGFP intensity profile SD distributions (normalized by counts for comparison) at the three aforementioned exposure times, showing increasing values of 136.8 $\pm$ 27.7 (mean $\pm$ SD), 159.0 $\pm$ 32.2, and 172.1 $\pm$ 34.8 nm, respectively.

and 175.5 nm, validating the notion that the SD provides a quantitative measure of the motion-induced blurriness of single fluorophore images.

In analytical calculations, we deduce an expression relating a diffusing eGFP's SD to D_{3D}. We first project the eGFP PSFs at all focal depths onto a 2D imaging screen, forming an axial-direction-projected PSF $f(x,y)$, and then convolve this projected PSF with the lateral location distribution of the molecule in a trajectory, which we define as a pathway distribution function ($PWDF_{x,y}$) in the lateral directions $g(x,y)$:

$$I(x,y) \propto f(x,y) * g(x,y). \tag{2}$$

Below, we decompose an eGFP's 3D diffusion process into two components for the s_x and D_{3D} calculation: a 1D diffusion along the axial direction, and a 2D diffusion in the lateral direction.

It is known that as the defocusing distance between the fluorophore and the focal plane increases, so does the SD of the PSF. Consequently, to calculate the intensity profile, one must integrate over all axial locations to which the molecule may have traveled during the exposure time to obtain an axial-direction-projected PSF, $f(x,y)$. Because diffusion values in the lateral and axial dimensions are statistically independent of each other, we choose to perform this integration before convolving the resulting PSF with $PWDF_{x,y}$ in the lateral dimensions to obtain the final projected 2D intensity profile of the 3D diffusing molecule on an imaging screen.

In the axial direction, we compute the axial-direction-projected PSF by numerically integrating defocused PSFs through z for all pixelated x, y-values:

$$\int_0^{400} C(z) e^{\left[-\frac{x^2}{2s_x(z)^2} - \frac{y^2}{2s_y(z)^2} - \frac{(z-\langle z_0\rangle)^2}{2A_z \cdot 2D_{3D}t} - \frac{z}{d}\right]} dz, \tag{3}$$

where $D_{3D} = 8.86 \times 10^7$ nm^2/s is the FCS-determined eGFP diffusion coefficient (Appendix S3); $C(z)$ and

$s_{x,y}(z)$ are the amplitude and SDs of our imaged, defocused eGFP Gaussian PSFs (Appendix S5), respectively; z_0 and $A_z \cdot 2D_{3D}t$ are the mean and variance of the diffusing eGFPs' Gaussian PWDF$_z$s (Appendix S7); $\exp(-z/d)$ describes the decaying TIRF evanescent excitation intensity; and the range for the z integration is the imaging depth of 0–400 nm measured from the focal point at the fused-silica surface. The resulting axial-direction-projected PSF $f(x,y)$ remains Gaussian, and the SD $s_0'(t)$ is a function of the exposure time t as $s_0'(t) = \sqrt{111^2 + 0.0634D_{3D}t}$ nm, where 111 nm and 0.0634 are fitted values.

In the lateral directions, we numerically calculate $g(x,y)$ of a freely diffusing eGFP particle by simulations. Fig. 4 *A* shows nine random PWDF$_x$s at exposure time t = 0.6 ms. Six of the nine PWDF$_x$s have one peak (unipeaked or unimodal) and can be fitted to a Gaussian function with $R^2 > 0.8$. Fig. 4 *B* shows the SD distribution of PWDF$_x$s, combining the Gaussian fitted SD values for the unipeaked PWDF$_x$s and the numerical particle location distribution SD values for the double-peaked PWDF$_x$s (mean = 96.8 nm). Fig. 4 *C* shows that when the nine PWDF$_x$s in Fig. 4 *A* are convolved with single-eGFP PSFs at focus with s_0 = 108.2 nm, all convolved PWDF$_x$s fit well to a Gaussian function, and the mean of the SD distribution is 147.1 nm. Therefore, although not all PWDF$_x$s are unipeaked, taken over all, we can view PWDF$_x$s as Gaussian functions with an average t-dependent SD value of $\sqrt{A_x \cdot 2D_{3D}t}$. For the 0.6 ms exposure time data, A_x = 0.0882. We found A_x to be insensitive to exposure times < 1 ms (mean A_x = 0.0926).

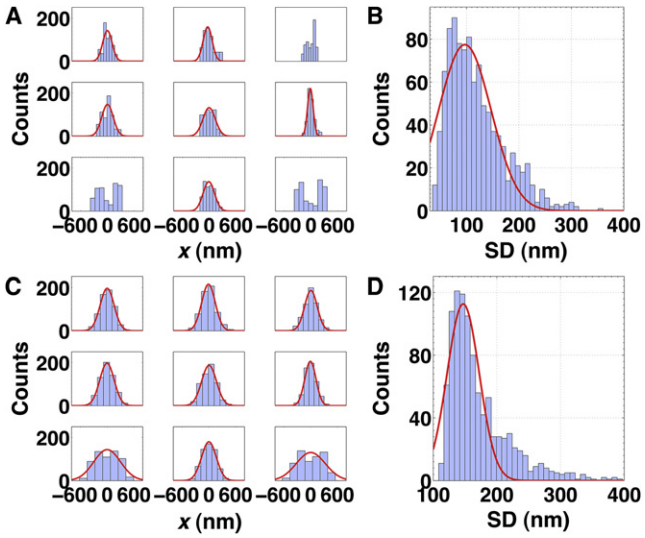

FIGURE 4 Study of the eGFP lateral PWDF$_x$s and their convolution with PSFs. (*A*) Nine random eGFP PWDF$_x$s at 0.6 ms exposure time and Gaussian fits to the unimodal distributions with $R^2 > 0.8$. (*B*) The distribution of 1000 PWDF$_x$ SDs, fitted with a Gaussian. (*C*) The nine PWDF$_x$s in (*A*) convolved with eGFP PSFs at focus with s_0 = 108.2 nm. (*D*) The SD distribution of 1000 PWDF$_x$ convolved eGFP PSFs at focus and its Gaussian fit.

Given that $f(x,y)$ (at focus and the axial-direction-projected) and $g(x,y)$ are both Gaussian functions, in the lateral directions their convolution can be described by another Gaussian function with a variance equal to the sum of the two variances. Using the focused eGFP PSFs with s_0 = 108.2 nm and PWDF$_x$ at 0.6 ms, the lateral direction SD value $s_{x,2D} = \sqrt{s_0^2 + A_x \cdot 2D_{3D}t} = \sqrt{108.2^2 + 96.8^2}$ nm = 145.2 nm, which is very close to the mean SD value of the above PSF-convolved-PWDF$_x$s of 147.1 nm.

Because we have observed that both the axial-direction-projected PSFs and the lateral PWDF$_{x,y}$s are Gaussian, the final projected intensity profiles' SD of diffusing molecules is

$$s_{x,y} = \sqrt{s_0'^2 + A_{x,y} \cdot 2D_{3D}t}, \tag{4}$$

where $s_0'(t) = \sqrt{111^2 + 0.0634D_{3D}t} \approx \sqrt{s_0^2 + 0.0634D_{3D}t}$ nm is the SD of the axial-direction-projected PSFs for our experimental parameters, and $A_{x,y} \cdot 2D_{3D}t$ is the variance of PWDF$_{x,y}$s with $A_{x,y}$ = 0.0926. This relation enables one to determine D_{3D} from the SD of a single-molecule's intensity profile and the exposure time as

$$D_{3D} = \frac{s_{x,y}^2 - s_0^2}{(2A_{x,y} + 0.0634)t}. \tag{5}$$

When the particle is diffusing in the 2D xy plane or along the 1D x or y axis, the 0.0634 term should be removed.

Using FCS-determined eGFP $D_{3D} = 8.86 \times 10^7$ nm^2/s in Eq. 4, we plot the analytical eGFP s_x results in Fig. 5 *A* and compare them with the experimental mean eGFP SD values

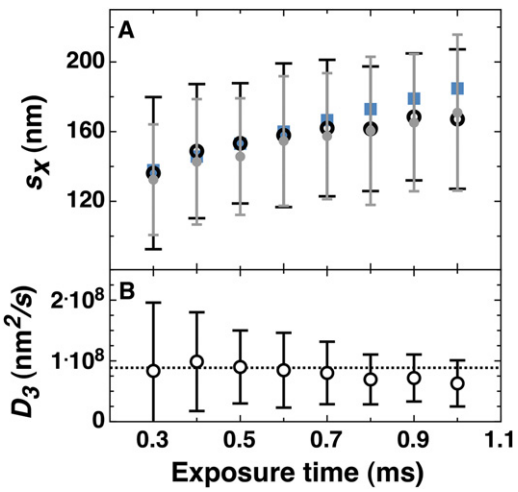

FIGURE 5 Comparing s_x and D_{3D} results. (*A*) Experimental (*circles*), simulation (*disks*), and theoretical calculation (*squares*) measurements of diffusing eGFP intensity profiles' mean s_x versus t. In the experimental and simulation results, the error bars are the SDs of the s_x distributions. (*B*) Experimental D_{3D} calculated from Eq. 5. The error bars are ΔD_{3D} calculated using Eq. 6; the dashed line is the FCS-determined eGFP D_{3D} of 8.86×10^7 nm^2/s for comparison.

obtained from Fig. 3 *B*, where the error bars are the SDs of the eGFP intensity profile SD distributions in Fig. 3 *B*. The analytical and experimental results show excellent agreement within 0.7 ms. Note that s_x starts to deviate from the experimental results at $t > 0.8$ ms; this is because the exposure time begins to approach the diffraction-limit-determined value for eGFP for this study (Appendix S1).

In simulations of diffusing eGFP intensity profiles (as shown in Fig. 2), we used the FCS-determined D_{3D}. Fig. 5 *A* juxtaposes the simulated diffusing eGFP SD results with the experimental results; the two mean values and error bars agree at all exposure times (Fig. S4 compares the results at $t = 0.6$ ms).

To determine the precision of the measured D_{3D} from single eGFP images, we performed an error propagation analysis of $D_{3D}(s_{x,y})$ using Eq. 5:

$$\Delta D_{3D} = \frac{s_{x,y}}{(A_{x,y} + 0.032)t}\Delta s_{x,y}, \quad (6)$$

where $\Delta s_{x,y}$ is the SD measurement precision of the single fluorophore's intensity profile (i.e., the experimental error bars in Fig. 5 *A*) (22). Fig. 5 *B* compares the experimentally determined D_{3D} and ΔD_{3D} from single diffusing eGFP image SD measurements with the FCS-determined eGFP $D_{3D} = 8.86$ nm^2/s, showing agreement.

At 0.7 ms, $\Delta D_{3D} = 5.2 \times 10^7$ nm^2/s for a single eGFP image using both the statistically independent mean s_x- and s_y-values of $s_{x,y} = 162.1$ nm and $\Delta s_{x,y} = 39.2$ nm. It is 57% of the eGFP D_{3D} of 8.86×10^7 nm^2/s. Because there are ~30 molecules in a typical frame image of <1 ms exposure time, the precision of the D_{3D} measurement further improves by $\sqrt{30}$ times to 10%, which is comparable to the precision of the FCS D_{3D} measurements (11). In spatially restrictive situations, such as in vivo imaging in typically micron-sized cells, where only one image can be obtained at a time, repeated single-image measurements will enable a precise determination of D_{3D}.

DISCUSSION

Although in this study we focused on fast diffusion of nanometer-sized proteins in free solution with $D_{3D} > 5 \times 10^7$ nm^2/s, our methodology applies to 3D diffusion at all rates. When diffusion coefficients are low for large particles, in a crowded environment, or in viscous solvents (such as in cells (23) or glycerol), the molecule's intensity profile will be more localized. Consequently, one should use longer exposure times to observe noticeable changes in the SD from the stationary values. Appendix S1 and Appendix S2 explain the procedure used to determine the appropriate exposure times for a particle of unknown D_{3D}.

In anisotropic environments where D_{1D}-values along the x and y axes differ, our separate D_{1D} measurements along the two lateral directions allow for such differentiation. If the diffusion coefficient differs along the axial direction, recalculation of Eq. 3 with new D_z- and A_z-values will still allow for determination of D_x and D_y using Eq. 5.

In certain cases, the molecules' movements can deviate from 3D unbiased Brownian motion (e.g., directional motion or diffusion with a drift). In future extension studies of these alternative motions using our single-image-based method, investigators should determine s_0' and $\mathrm{PWDF}_{x,y,z}$ before convolving the axial-direction-projected PSF with $\mathrm{PWDF}_{x,y}$ for the final intensity profile. As long as the mean numerical SD of locations in the molecule's trajectory is less than half of the diffraction limit at the exposure time, the projected convolved image of the molecule will be a unimodal intensity profile that can be fitted to a Gaussian function, and the resulting $s_{x,y}$ will provide information about the molecule's dynamics.

In summary, we have presented a new (to our knowledge) single-molecule fluorescence image analysis method that measures fast diffusion coefficients with high precision. The experimental setup and data analysis are simple to use with standard microscopy imaging systems, and the method is applicable to a wide range of diffusion coefficient measurements with greatly improved temporal resolution. Applications to basic research and pharmaceutical investigations, such as fast drug screening, can be envisioned.

SUPPORTING MATERIAL

Document S1. Six figures, seven appendices, and references (24–30) are available at http://www.biophysj.org/biophysj/supplemental/S0006-3495(12)00261-5.

REFERENCES

1. Wang, Y. M., R. H. Austin, and E. C. Cox. 2006. Single molecule measurements of repressor protein 1D diffusion on DNA. *Phys. Rev. Lett.* 97:048302.

2. Gorman, J., and E. C. Greene. 2008. Visualizing one-dimensional diffusion of proteins along DNA. *Nat. Struct. Mol. Biol.* 15:768–774.

3. Thompson, M. A., M. D. Lew, …, W. E. Moerner. 2010. Localizing and tracking single nanoscale emitters in three dimensions with high spatiotemporal resolution using a double-helix point spread function. *Nano Lett.* 10:211–218.

4. Auer, M., K. J. Moore, …, K. A. Stoeckli. 1998. Fluorescence correlation spectroscopy: lead discovery by miniaturized HTS. *Drug Discov. Today.* 3:457–465.

5. Ganser, A., G. Roth, …, R. Brock. 2009. Diffusion-driven device for a high-resolution dose-response profiling of combination chemotherapy. *Anal. Chem.* 81:5233–5240.

6. He, L., and B. Niemeyer. 2003. A novel correlation for protein diffusion coefficients based on molecular weight and radius of gyration. *Biotechnol. Prog.* 19:544–548.

7. Webb, G. A. 2005. Nuclear Magnetic Resonance., Vol. 34. Royal Society of Chemistry, Cambridge, UK.

8. Berne, B., and R. Pecora. 2000. Dynamic Light Scattering: With Application to Chemistry, Biology and Physics. General Publishing Company, Toronto, Ontario, Canada.

9. Magde, D., E. Elson, and W. W. Webb. 1972. Thermodynamic fluctuations in a reacting system - measurement by fluorescence correlation spectroscopy. *Phys. Rev. Lett.* 29:705–708.

10. Schenk, A., S. Ivanchenko, …, G. U. Nienhaus. 2004. Photodynamics of red fluorescent proteins studied by fluorescence correlation spectroscopy. *Biophys. J.* 86:384–394.

11. Petrásek, Z., and P. Schwille. 2008. Precise measurement of diffusion coefficients using scanning fluorescence correlation spectroscopy. *Biophys. J.* 94:1437–1448.

12. Potma, E. O., W. P. de Boeij, …, D. A. Wiersma. 2001. Reduced protein diffusion rate by cytoskeleton in vegetative and polarized dictyostelium cells. *Biophys. J.* 81:2010–2019.

13. Blainey, P. C., A. M. van Oijen, …, X. S. Xie. 2006. A base-excision DNA-repair protein finds intrahelical lesion bases by fast sliding in contact with DNA. *Proc. Natl. Acad. Sci. USA.* 103:5752–5757.

14. Nachury, M. V., E. S. Seeley, and H. Jin. 2010. Trafficking to the ciliary membrane: how to get across the periciliary diffusion barrier? *Annu. Rev. Cell Dev. Biol.* 26:59–87.

15. Ritchie, K., and J. Spector. 2007. Single molecule studies of molecular diffusion in cellular membranes: determining membrane structure. *Biopolymers.* 87:95–101.

16. Qian, H., M. P. Sheetz, and E. L. Elson. 1991. Single particle tracking. Analysis of diffusion and flow in two-dimensional systems. *Biophys. J.* 60:910–921.

17. Levi, V., Q. Ruan, and E. Gratton. 2005. 3-D particle tracking in a two-photon microscope: application to the study of molecular dynamics in cells. *Biophys. J.* 88:2919–2928.

18. Semrau, S., A. Pezzarossa, and T. Schmidt. 2011. Microsecond single-molecule tracking (μsSMT). *Biophys. J.* 100:L19–L21.

19. DeCenzo, S. H., M. C. DeSantis, and Y. M. Wang. 2010. Single-image separation measurements of two unresolved fluorophores. *Opt. Express.* 18:16628–16639.

20. Schuster, J., F. Cichos, and C. von Borczyskowski. 2002. Diffusion measurements by single-molecule spot-size analysis. *J. Phys. Chem. A.* 106:5403–5406.

21. Zareh, S. K., and Y. M. Wang. 2011. Single-molecule imaging of protein adsorption mechanisms to surfaces. *Microsc. Res. Tech.* 74:682–687.

22. DeSantis, M. C., S. H. DeCenzo, …, Y. M. Wang. 2010. Precision analysis for standard deviation measurements of immobile single fluorescent molecule images. *Opt. Express.* 18:6563–6576.

23. Swaminathan, R., C. P. Hoang, and A. S. Verkman. 1997. Photobleaching recovery and anisotropy decay of green fluorescent protein GFP-S65T in solution and cells: cytoplasmic viscosity probed by green fluorescent protein translational and rotational diffusion. *Biophys. J.* 72:1900–1907.

24. Weisshart, K., V. Jüngel, and S. J. Briddon. 2004. The LSM 510 META-ConfoCor 2 system: an integrated imaging and spectroscopic platform for single-molecule detection. *Curr. Pharm. Biotechnol.* 5:135–154.

25. Willig, K. I., R. R. Kellner, …, S. W. Hell. 2006. Nanoscale resolution in GFP-based microscopy. *Nat. Methods.* 3:721–723.

26. Egner, A., and S. W. Hell. 1999. Equivalence of the Huygens–Fresnel and Debye approach for the calculation of high aperture point-spread functions in the presence of refractive index mismatch. *J. Microsc.* 193:244–249.

27. Huang, B., W. Wang, …, X. Zhuang. 2008. Three-dimensional super-resolution imaging by stochastic optical reconstruction microscopy. *Science.* 319:810–813.

28. Yildiz, A., J. N. Forkey, …, P. R. Selvin. 2003. Myosin V walks hand-over-hand: single fluorophore imaging with 1.5-nm localization. *Science.* 300:2061–2065.

29. Yildiz, A., M. Tomishige, …, P. R. Selvin. 2004. Kinesin walks hand-over-hand. *Science.* 303:676–678.

30. Axelrod, D. 1989. Total internal reflection fluorescence microscopy. *Methods Cell Biol.* 30:245–270.